Journal of Physics: Conference Series **2919** (2024) 012024 doi:10.1088/1742-6596/2919/1/012024

Large Kerr Nonlinearity and Slow Group Velocity of Weak Probe in Quantum Dot Nanostructures

Minhaz Al Hussain[1*], Thulunga Basumatary[1], Abhijit Shyam[1], Rohit Mukherjee[2], and Nitu Borgohain[1]

[1]Department of Physics, University of Science & Technology, Meghalaya (USTM), Meghalaya, India-793101

[2]Theoretical Photonics Group, Department of Physics, Sarala Birla University, Jharkhand, India-835103

[*]E-mail: laurathussain2332@gmail.com

Abstract:

This paper presents the dynamics of Kerr nonlinearity and the phenomenon of slow group velocity in a Quantum Dot (QD) system, using the mechanism of electromagnetically induced transparency (EIT). Employing a three-level QD setup and leveraging a ladder-type excitation approach, we analyse the interaction between a weak probe pulse and a strong control beam. By employing density matrix formalism, we derive the expressions for both linear and nonlinear optical susceptibilities, along with first-order linear dispersion terms. Our findings reveal that susceptibilities in the QD system, both linear and nonlinear, can be finely adjusted to desired probe frequencies through control parameter manipulation. Moreover, under the EIT regime, we observe the Kerr susceptibility on the order of 10^{-12} m^2/V^2 at a probe wavelength 1.359 μm. Additionally, the group velocity of the probe field experiences a remarkable slowdown by a factor of 10^3 compared to the speed of light in vacuum. Results obtained may have potential applications in fabricating nonlinear optical devices.

1. INTRODUCTION

In recent years, QD nanostructures have emerged as significant players in the field of nonlinear optics due to their unique electronic and optical properties [1-5]. Among the fascinating phenomena exhibited by these structures, large Kerr nonlinearity and slow group velocity are emerged as the key effects that advantage them from other materials. These properties are critical for the development of advanced photonic devices such as optical switches, modulators, and slow-light systems [6-10]. In QD nanostructures, the Kerr nonlinearity can be significantly enhanced due to quantum confinement effects, which leads to discrete energy levels and enhanced dipole moments, which in turn increase the nonlinear optical response [11-13]. Recent studies have shown that the magnitude of Kerr nonlinearity in QDs can be several orders of magnitude higher than in bulk materials. For example, colloidal CdSe quantum dots embedded in glass matrices have demonstrated a Kerr coefficient significantly larger than that of traditional materials [14].

In QD nanostructures, the effect of slow light can be achieved at very large magnitude. Slow light refers to the reduction of the group velocity of light as it propagates through a medium, and it can be achieved in QDs through coherent population oscillations, electromagnetically induced transparency

(EIT), and other quantum coherence effects [15-19]. The slow group velocity is highly beneficial for enhancing light-matter interactions, which is crucial for developing efficient optical buffers and enhancing the performance of nonlinear optical devices.

Despite the promising properties and applications, there are several challenges to be addressed. These include the precise control of absorption and dispersion, under EIT scheme, which may lead to efficient Kerr nonlinearity and slow group velocity with high sensitivity, in QD nanostructures. In this article, we investigate large Kerr nonlinearity and slowing down of a weak probe pulse, controlled by a strong laser beam, under an EIT regime.

The article is arranged as follows: In section 2 we present the theoretical model and governing equations, section 3 deals the discussion on Kerr nonlinearity and slow group velocity, under EIT. A summary of the results is included in section 4.

2. PHYSICAL MODEL AND GOVERNING EQUATIONS

We examine a three-level quantum dot system, GaAs–InGaAs–InAs, where the dot is hypothesized as a quantum disk with a radius (a) of 9 nm and a height (h) of 3.5 nm. [20]. The energy level diagram along with the transitions is presented in figure 1. In this quantum dot system, a weak probe pulse characterized by an angular frequency ω_p stimulates the transition from state $|1\rangle$ to state $|2\rangle$, and a strong control beam characterized by angular frequency ω_c drives the transition from state $|2\rangle$ to state $|3\rangle$, in a ladder-type configuration. The energies associated with the states are $E_{21} = 0.91$ eV and $E_{32} = 0.096$ eV.

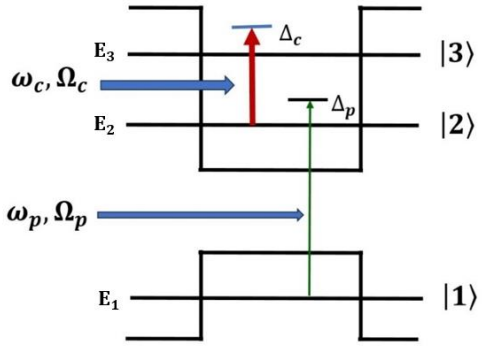

Figure 1: Diagram illustrating the energy levels in a ladder-type excitation arrangement of the Quantum Dot system.

For this system, the semi-classical form of Hamiltonian can be expressed as

$$\hat{H} = (\hbar\omega_1|1\rangle\langle 1| + \hbar\omega_2|2\rangle\langle 2| + \hbar\omega_3|3\rangle\langle 3|) - \hbar\{\Omega_p e^{-i\omega_p t}|2\rangle\langle 1| + \Omega_c e^{-i\omega_c t}|3\rangle\langle 2| + \Omega_p^* e^{i\omega_p t}|1\rangle\langle 2| + \Omega_c^* e^{i\omega_c t}|2\rangle\langle 3|\} \quad (1)$$

where $\hbar\omega_1$ and $\hbar\omega_2$ represents the energy associated with the states $|1\rangle$ and $|2\rangle$ respectively of the QD structure. The Rabi frequencies, Ω_p and Ω_c, are for the laser driven interband transitions between

states $|1\rangle$ and $|2\rangle$ and intersubband transition between states $|2\rangle$ and $|3\rangle$, respectively. They can be stated precisely in the following manner: $\Omega_p = \frac{\mu_{21}E_p}{\hbar}$ and $\Omega_c = \frac{\mu_{32}E_c}{\hbar}$.

The density matrix equations of motion after removing the oscillating terms for the system can be written as follows,

$$\frac{\partial}{\partial t}\tilde{\rho}_{21} = i\left(\Delta_p + i\frac{\gamma_{21}}{2}\right)\tilde{\rho}_{12} + i\Omega_p(\tilde{\rho}_{11} - \tilde{\rho}_{22}) + i\Omega_c^*\tilde{\rho}_{31}, \quad (2)$$

$$\frac{\partial}{\partial t}\tilde{\rho}_{31} = i\left[(\Delta_p + \Delta_c) + i\frac{\gamma_{31}}{2}\right]\tilde{\rho}_{31} + i\Omega_c\tilde{\rho}_{21} - i\Omega_c\tilde{\rho}_{32}, \quad (3)$$

$$\frac{\partial}{\partial t}\tilde{\rho}_{32} = i\left(\Delta_c + i\frac{\gamma_{32}}{2}\right)\tilde{\rho}_{31} + i\Omega_c(\tilde{\rho}_{22} - \tilde{\rho}_{33}) + i\Omega_p^*\tilde{\rho}_{31}. \quad (4)$$

Here the intersubband transition detunings are defined as $\Delta_p = \omega_p - \frac{E_2 - E_1}{\hbar}$ and $\Delta_c = \omega_c - \frac{E_3 - E_2}{\hbar}$ and γ_{21}, γ_{31} are the population decay rates.

For a nonlinear material, the susceptibility can be separated into two segments, the first part is linear and the other part is nonlinear. This can be written in the following manner: $\vec{P} = \epsilon_0\{\chi^{(1)}\vec{E} + \chi^{(3)}|\vec{E}|^2\}$, where we have considered the terms up to the third order only.

The susceptibilities at the probe frequency, both for first and third order, can be expressed as follows:

$$\chi^{(1)} = -\frac{N|\mu_{21}|^2}{\epsilon_0\Omega_p\hbar}\frac{D_p(0)}{D(0)}, \quad (5)$$

$$\chi^{(3)} = \frac{N|\mu_{21}|^4}{4\epsilon_0\hbar^3}\left\{\frac{(|\Omega_1|^2 + |D_p(0)|^2)D_p(0)}{|D(0)|^2 D(0)}\right\}, \quad (6)$$

where $D_p(0) = (\Delta_p + \Delta_c + i\frac{\gamma_{31}}{2})$ and $D(0) = \{\left(\Delta_p + i\frac{\gamma_{21}}{2}\right)\left(\Delta_p + \Delta_c + i\frac{\gamma_{31}}{2}\right) - |\Omega_c|^2\}$.

At this stage we have discussed the expressions of the linear and nonlinear optical susceptibilities of the quantum dot.

The propagation constant of the probe pulse is given by

$$K(\omega) = \frac{\omega}{c} - \alpha\frac{D_p(\omega)}{D(\omega)}, \quad (7)$$

Where, $\alpha = \frac{N|\mu_{21}|^2\omega_p}{2\hbar\epsilon_0 c}$, N is the carrier density, $D_p(\omega) = (\omega + \Delta_p + \Delta_c + i\frac{\gamma_{31}}{2})$ and $D(0) = \{\left(\omega + \Delta_p + i\frac{\gamma_{21}}{2}\right)\left(\omega + \Delta_p + \Delta_c + i\frac{\gamma_{31}}{2}\right) - |\Omega_c|^2\}$.

The expression for $K(\omega)$ can be represented as a Taylor series centred around the central frequency of the probe field ($\omega = 0$) as:

$$K(\omega) = K(0) + K_1(0)\omega + \frac{1}{2}K_2(0)\omega^2 + \cdots \quad (8)$$

The values of $K^n(0)s$ are achieved in this manner: $K^n(0) = \left.\frac{d^nK}{d\omega^n}\right|_{\omega=0}$, this gives us

$$K(0) = -\alpha \frac{D_p(\omega)}{D(\omega)} \text{ and} \tag{9}$$

$$K_1 = \frac{1}{c} + \left[\frac{\alpha}{|\Omega_c|^2 - -\left[\Delta_p + i\frac{\gamma_{21}}{2} + \omega\right]\left[\Delta_c + \Delta_p + i\frac{\gamma_{31}}{2} + \omega\right]}\right] + \left[\frac{\alpha\left\{\Delta_c + \Delta_p + i\frac{\gamma_{31}}{2} + \omega\right\}}{[|\omega_c|^2 - (\Delta_p + \omega + i\frac{\gamma_{21}}{2})(\Delta_c + 2\Delta_p + i\frac{\gamma_{31}}{2})]^2}\right] \tag{10}$$

In our work we restrict only up to the first order dispersion term $K(\omega)$ as our concern is only with the group velocity which is given by $V_g = \text{Re}\left[\frac{1}{K_1(0)}\right]$. Now we are ready to examine the linear susceptibility and group velocity of the probe pulse, considering the diverse parameters linked with the QD.

3. RESULTS AND DISCUSSIONS

This section introduces the findings of the first-order (linear) and third-order (nonlinear) susceptibilities under the conditions of electromagnetically induced transparency (EIT). Concerning the exploration, we have taken the system parameters as follows: $N = 1.14 \times 10^{23} m^{-3}$, $\mu_{21} = 33.6 \times 10^{-29}$ mC, $\hbar = 1.05 \times 10^{-34} Js$, $\epsilon_0 = 8.854 \times 10^{-12}\ C^2N^{-1}m^2$, and the decay terms are $\gamma_{21} = 0.243 \times 10^{10}\ s^{-1}$ and $\gamma_{31} = 8.04 \times 10^{10}\ s^{-1}$. The imaginary component of the first-order susceptibility, Im $\chi^{(1)}$, illustrates the linear absorption, while the real part, Re $\chi^{(1)}$, signifies the linear dispersion of the system. Figure 2 illustrates the behavior of these components. In figure 2(a), the profile of Im $\chi^{(1)}$ concerning the probe detuning (Δ_p), indicates that when the control field is absent ($\Omega_c = 0$), the probe field experiences significant absorption at resonance ($\Delta_p = 0$). As we switch on the control field and continue to increase its value, at first, the absorption peak starts diminishing and later, it splits into two creating an EIT window. The window keeps on increasing as the intensity of the control field is increased. Also, from the figure 2(b), which portrays Re $\chi^{(1)}$ with respect to Δ_p, we observe that when the control field is not applied ($\Omega_c = 0$), there is a negative slope indicating the dispersion to be anomalous. When the control field is applied ($\Omega_c > 0$), the Re $\chi^{(1)}$ possesses a positive slope signifying the dispersion to be normal. This reveals that the dispersion can be toggled between normal to anomalous and vice-versa, by manipulating the control field.

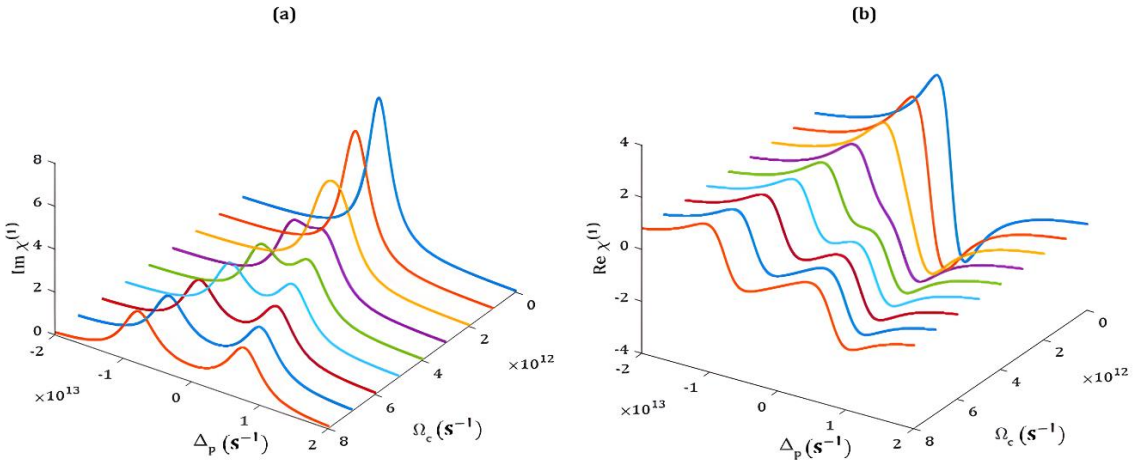

Figure 2: Changes in linear susceptibility as a function of probe detuning. (a) Imaginary, and (b) real part of $\chi^{(1)}$ for a range of control field Rabi frequency.

Next, we investigate the behaviour of the nonlinear susceptibility ($\mathrm{Re}\,\chi^{(3)}$) as a function of Δ_p for different values of Ω_c, which is depicted in figure 3. The graph reveals that with smaller values of ($\Omega_c \approx 0$), only one peak is observed. However, as Ω_c increases, the peak of the $\mathrm{Re}\,\chi^{(3)}$ profile splits into two parts, with the gap widening as Ω_c rises. By plotting the graph of $\mathrm{Re}\,\chi^{(3)}$, it has been observed that inside the transparency window a large Kerr nonlinearity of the order $10^{-12}\,\mathrm{m}^2/\mathrm{V}^2$ is obtained. Hence, it becomes evident that the Kerr nonlinearity displayed within the EIT window is very large which could be tuned to any desired probe frequency by manipulating the Rabi frequency of the control field. At this stage, it is worthy to compare the values of Kerr nonlinearities possess by different materials. Table-1 shows a few semiconductor materials with their nonlinear susceptibilities placed for comparison with our proposed work. It is seen that the system adopted for this study possesses much higher value than others.

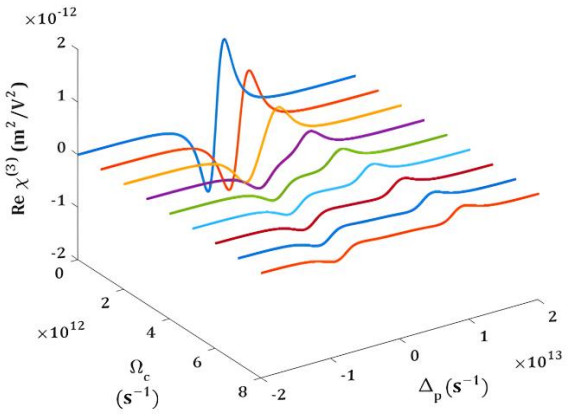

Figure 3: Changes in the real component of $\chi^{(3)}$ concerning the probe detuning, across a range of control field Rabi frequencies.

Table-1: Comparison of nonlinear susceptibilities of different materials

Material	Nonlinear Susceptibility	Reference
Fused silica	$1.9 \times 10^{-22}\,\mathrm{m}^2/\mathrm{V}^2$	[17]
Semiconductor dopped glass fiber	$4.5 \times 10^{-19}\,\mathrm{m}^2/\mathrm{V}^2$	[18]
InGaAs/AlAs/AlAsSb	$5.8 \times 10^{-17}\,\mathrm{m}^2/\mathrm{V}^2$	[19]
Semiconductor QD	$1.0 \times 10^{-12}\,\mathrm{m}^2/\mathrm{V}^2$	Present Paper

Now, we investigate the dynamics reduced group velocity of the probe field under the control field effect. In figure 4, we show the reliance of the probe pulse's normalized group velocity ($\mathrm{V_g}/\mathrm{c}$) for different values of $\Omega_c = (0-8) \times 10^{12}\mathrm{s}^{-1}$. When $\Omega_c = 0$, the group velocity experiences an initial decrease, reaches a minimum, and then increases with Δ_p. For $\Omega_c = 3 \times 10^{12}\mathrm{s}^{-1}$ and $\Omega_c = 3.5 \times 10^{12}\mathrm{s}^{-1}$, the initial decrease in $\mathrm{V_g}/\mathrm{c}$ is followed by a small deep around $\Delta_p = 0$, after which it increases with Δ_p. At $\Omega_c = 5 \times 10^{12}\mathrm{s}^{-1}$, there appears a hump at around $\Delta_p = 0$ in the $\mathrm{V_g}/\mathrm{c}$ profile, which goes on widen with further increase of Ω_c.

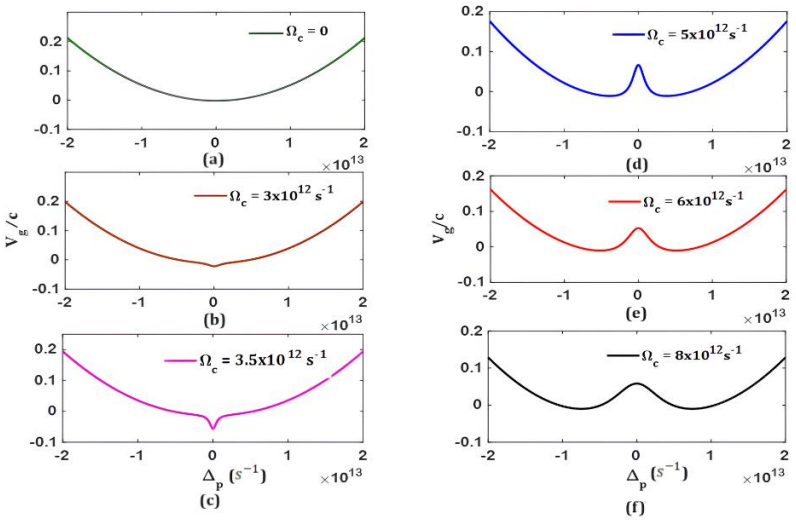

Figure 4: Variation of normalized V_g/c with probe detuning for different values of Ω_c. (a) $\Omega_c = 0$, (b) $\Omega_c = 3x10^{12}$ s^{-1}, (c) $\Omega_c = 3.5x10^{12}$ s^{-1}, (d) $\Omega_c = 5x10^{12}$ s^{-1}, (e) $\Omega_c = 6x10^{12}$ s^{-1}, and (f) $\Omega_c = 8x10^{12}$ s^{-1}. Also, the control detuning is set at $\Delta_c = 0$.

Following this, we study the effect of the control field detuning on the normalized group velocity, as depicted in figure 5. Figure 5(a) gives the surface plot of the V_g/c with Δ_p for a range of different values of Δ_c. The central green line represents the hump, which shifts towards the negative side of the probe detuning on increasing the Δ_c values. Figure 5 (b) shows the line plots of V_g/c as a function Δ_p for a few values of Δ_c. When $\Delta_c = 0$, the hump is at the centre, as seen in the top panel of figure 5(b), but with increase Δ_c, the hump shifts towards the negative side of the probe detuning. From the bottom panel of figure 5(b) it is seen that for $\Delta_c = 4 \times 10^{12} s^{-1}$, at probe detuning $\Delta_p = 3.2 \times 10^{12} s^{-1}$, the group velocity is found to be about $V_g = 1.2 \times 10^5$ m/s. This group velocity is significantly smaller, about 10^3 times, than the speed of light in vacuum. Thus, it is confirmed that both control field intensity as well as detuning can shift the group velocity profile to any desired probe frequency point.

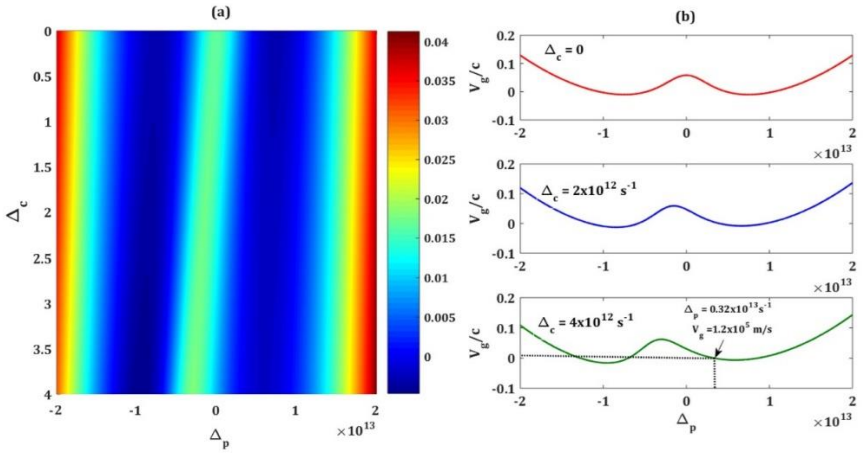

Figure 5: Variation in V_g/c concerning Δ_p aimed at different values of Δ_c. Here, Ω_c is kept at constant value at 8×10^{12} s^{-1}.

4. CONCLUSION

In conclusion, our exploration into the dynamics of slow group velocity within a weak probe field influenced by a control field within an electromagnetically induced transparency (EIT) window, in a quantum dot (QD) nanostructure employing a ladder-type configuration, has yielded insightful findings. Specifically, we have uncovered a significant Kerr nonlinear susceptibility, approximately of the order of $\sim 10^{-12}\,\mathrm{m}^2/\mathrm{V}^2$, within the QD system, facilitated by the EIT-induced low absorption. This EIT window affords the probe pulse a considerably slower propagation compared to scenarios without the control field. Remarkably, we have observed that the group velocity of the probe laser pulse experiences a deceleration by a factor of 10^3 compared to the speed of light in vacuum. These outcomes suggest promising avenues for potential applications in optical information engineering within solid systems.

5. ACKNOWLEDGEMENT

Authors acknowledge the moral and infrastructure support from Shri M. Hoque, Chancellor of USTM, Meghalaya with thanks.

REFERENCES

[1] J. M. Pietryga, Y. S. Park, J. Lim, A. F. Fidler, W. K. Bae, S. Brovelli, & V. I. Klimov, (2016), Chemical Reviews, **116**, 10513-10622.
[2] X. Liu, Q. Guo, & J. Qiu, (2017), Advanced Materials, **29**, 1605886.
[3] M. J. Smith, C. H. Lin, S. Yu, & V. V. Tsukruk, (2019), Advanced Optical Materials, 7, 1801072.
[4] S. K. Sarkar, (2023), Quantum Dots as Optical Materials: Small Wonders and Endless Frontiers, In Handbook of Materials Science, Volume 1: Optical Materials, Singapore: Springer Nature Singapore, (pp. 545-596).
[5] X. Jiang, K. Guo, G. Liu, T. Yang, & Y. Yang, (2017), Superlattices and Microstructures, **105**, 56-64.
[6] K. Asakawa, Y. Sugimoto, Y. Watanabe, N. Ozaki, A. Mizutani, Y. Takata, & R. Baets, (2006), New Journal of Physics, **8**, 208.
[7] D. Pacifici, H. J. Lezec, & H. A. Atwater, (2007), Nature photonics, **1**, 402-406.
[8] A. Majumdar, N. Manquest, A. Faraon, & J. Vučković, (2010), Optics Express, **18**, 3974-3984.
[9] F. K. Hachim, B. O. Al-Nashy, & A. H. Al-khursan, (2023), Optical and Quantum Electronics, 55, 831.
[10] X. Chen, et al., (2023), Nature Photonics, **17**, 217-224.
[11] M. M. Tohari, A. Lyras, & M. S. AlSalhi, (2018), Nanomaterials, **8**, 521.
[12] P. Hosseinpour, (2021), Physica B: Condensed Matter, 613, 412973.
[13] S. C. Tian, R. G. Wan, C. Z. Tong, Y. Q. Ning, L. Qin, & Y. Liu, (2014), Journal of the Optical Society of America B, **31**, 1436-1442.
[14] G. Dong, H. Wang, G. Chen, Q. Pan, & J. Qiu, (2015), Frontiers in materials, **2**, 13.
[15] H. Zhang, et al., (2023), Optics Express, **31**, 1289-1296.
[16] Y. Liu, et al., (2022*),* Applied Physics Letters, **120**, 031105.
[17] Q. Wang, et al., (2023), Physical Review B, **107**, 054202.
[18] R. Kumar, et al., (2023), Journal of Lightwave Technology, **41**, 1956-1963.
[19] S. Lee, et al., (2023), ACS Photonics, **10**, 563-570.
[20] J Kim, Shun-Lien Chuang, Pei-Cheng Ku, Connie J Chan-Hasnain, (2004), Journal of Physics: Condensed Matter **16**, S3727.